Thank you very much for the constructive comments.

The comments are on description of errors and potential systematic bias for the determined values, discussion of the salting-out behavior observed, estimate of the amount of CH_2F_2 dissolved in the ocean mixed layer, and relation between dissolution of CH_2F_2 in the ocean and estimation of CH_2F_2 emissions in the Southern Hemisphere and its seasonal variability.

I will reply to each comment as follows. Parts of texts and numbers revised in the manuscript are marked in blue.

R1. Reply to the comment on discussion of experimental error. What are the parameters that limit the accuracy of the inert-gas stripping (IGS) method? Of the stripping column apparatus? And of the phase ratio variation headspace (PRV-HS) method? Do error bars reflect statistics only, or also potential sources of systematic bias?

Thank you for the comments.

I reply to the comments in the sequence: (1) on the parameters that limit the accuracy of the IGS method; (2) on the parameters that limit the accuracy of the PRV-HS method; and (3) on error bars.

(1) the parameters that limit the accuracy of the IGS methods

The parameters that limit the accuracy of the IGS methods are temperature of the test solution (T) and flow rate of purge gas (F).

The accuracy of T (δT) are within 0.2 K and may give potential systematic bias of ±0.5 to ±0.6 % ($\delta K_{eq}/K_{eq}$), where δK_{eq} indicates an error of K_{eq}.

For F, the accuracy of F_{meas} is estimated to be within 1% from the accuracy of the high-precision film flow meter SF-1U with VP-2U used for calibrating the soap flow meter. Errors in the term of $\frac{P_{meas}-h_{meas}}{P_{hs}-h} \times \frac{T}{T_{meas}}$ in Eq (3) are estimated at ca. ±1 %. Hence, the accuracy of F (δF) are estimated to be within 1.4 % and may give potential systematic bias of ±1.4 % of $\delta K_{eq}/K_{eq}$.

Values of $\delta K_{eq}/K_{eq}$ due to both δT and δF may thus have potential systematic bias of ca. ±2%.

(2) the parameters that limit the accuracy of the PRV-HS methods

The parameters that limit the accuracy of the PRV-HS methods are temperature of the test solution (T) and volume of the vials used (V).

Although the apparatus used (Agilent, HP7694) was expected to keep T constant, the accuracy of T may not be certified. I have applied the same apparatus to determination of the K_H values for some HCFCs such as HCFC-123 using the PRV-HS methods [Kutsuna, S. *Int. J. Chem. Kinet.*, 45, 440-451, 2013]. On the basis of the K_H values thus determined and comparison between them and the reported values for HCFC-123, errors of T are estimated to be within ca. 2 K. These errors of T may give potential systematic bias of ca. ±4 % ($\delta K_{eq}/K_{eq}$) at 313 K and ca. ±3 % ($\delta K_{eq}/K_{eq}$) at 353 K.

Errors for V (δV) are estimated to be less than 1 %, and these errors may give potential systematic bias of less than 1 % of $\delta K_{eq}/K_{eq}$.

Accordingly, for the PRV-HS methods, values of $\delta K_{eq}/K_{eq}$ due to both δT and δV may have potential systematic bias of ca. ±4%.

(3) Error bars in Figure 2

Error bars in Figure 2 reflect statics only (Error_S) in the original manuscript. Error bars in Figure 2m represent errors (Error_T) reflecting both Error_S and potential systematic bias (Error_B). Values of Error_T are also indicated in Tables 1m, S1m and 3m. Values of Error_T are calculated by (Error_S + Error_B) rather than $\sqrt{(\text{Error\_S})^2 + (\text{Error\_B})^2}$ because

Error_B is potential systematic bias.

Table 1m. The average of values of $F/(k_1RTV)$ obtained for V value of 0.350 dm^3 and 0.300 dm^3 and the $K_H(T)$ value derived from Eq. (13) at each temperature. N represents number of experimental runs for the average.

T (K)	$F/(k_1RTV)$				$K_H(T)$ (M atm^{-1})
	V = 0.350		V = 0.300		
	average [a, b]	N [c]	average [a]	N [c]	From Eq. (13) [d]
276.15	0.119 ± 0.006 (0.008)	21 (2)	0.117 ± 0.006 (0.008)	11 (0)	0.118 ± 0.003
278.35	0.107 ± 0.005 (0.007)	18 (3)	0.110 ± 0.005 (0.007)	14 (0)	0.108 ± 0.002
283.65	0.093 ± 0.003 (0.005)	27 (5)	0.092 ± 0.001 (0.003)	5 (0)	0.094 ± 0.002
288.65	0.082 ± 0.006 (0.008)	41 (5)	0.084 ± 0.006 (0.008)	12 (0)	0.082 ± 0.002
293.45	0.071 ± 0.001 (0.002)	15 (8)	0.071 ± 0.001 (0.002)	5 (0)	0.072 ± 0.002
298.15	0.064 ± 0.002 (0.003)	30 (6)	0.067 ± 0.005 (0.006)	12 (0)	0.064 ± 0.002
303.05	0.057 ± 0.003 (0.004)	16 (0)	0.056 ± 0.005 (0.006)	4 (0)	0.058 ± 0.002
307.95	0.051 ± 0.001 (0.002)	12 (6)	0.054 ± 0.004 (0.005)	10 (0)	0.052 ± 0.002
312.65	0.046 ± 0.001 (0.002)	13 (3)	0.047 ± 0.001 (0.002)	4 (0)	0.048 ± 0.001

a. Errors are 2σ for the average only.; b. Number in parenthesis represents an error reflecting both 2σ for the average and potential systematic bias.; c. Number in parenthesis represents number of experimental runs excluded for the average.; d. Errors are 95% confidence level for the regression only.

Table S1m. L_i values for various V_i/V_0 ratios at various temperatures, slopes and intercepts for linear regression with respect to Eq. (10), $K_H(T)$ values calculated from the slopes and intercepts, and $K_H(T)$ values and the errors at 95% confidence level estimated by non-linear fitting the two datasets simultaneously at each temperature (Fig. S4) with respect to Eq. (11).

T (K)	L_i (a.u.) [*]						Eq. (10) Intercept	Eq. (10) Slope	K_H (M atm^{-1})		
	V_i/V = 0.421	0.351	0.280	0.210	0.140	0.070			Eq. (10)	Eq. (11)[**, ***]	Eq. (13)[**]
353	3.226±0.002	3.270±0.026	3.330±0.004	3.391±0.008	3.462±0.014	3.526±0.009	3.581	–0.870	0.026	0.027 ±0.002 (±0.003)	0.031 ±0.003
	2.044±0.006	2.050±0.012	2.112±0.010	2.132±0.009	2.186±0.021	2.209±0.011	2.248	–0.513	0.027		
343	3.000±0.018	3.025±0.009	3.070±0.008	3.089±0.015	3.117±0.015	3.148±0.018	3.179	–0.423	0.031	0.031 ±0.001 (±0.002)	0.033 ±0.002
	1.949±0.004	1.955±0.005	1.968±0.003	1.998±0.004	2.020±0.002	2.030±0.009	2.050	–0.258	0.031		
333	3.247±0.018	3.234±0.018	3.243±0.015	3.241±0.010	3.247±0.009	3.223±0.013	3.231	0.034	0.037	0.036 ±0.003 (±0.004)	0.037 ±0.002
	3.080±0.009	3.044±0.006	3.082±0.005	3.127±0.009	3.113±0.008	3.134±0.014	3.149	–0.213	0.034		
323	3.208±0.011	3.190±0.008	3.133±0.010	3.134±0.011	3.092±0.008	3.093±0.006	3.055	0.355	0.042	0.043 ±0.002 (±0.004)	0.042 ±0.001
	3.357±0.010	3.289±0.014	3.275±0.005	3.233±0.004	3.226±0.016	3.160±0.001	3.135	0.496	0.044		
313	3.245±0.018	3.185±0.013	3.100±0.015	3.022±0.012	2.995±0.012	2.915±0.011	2.848	0.935	0.052	0.052 ±0.003 (±0.005)	0.049 ±0.001
	2.162±0.031	2.134±0.010	2.060±0.014	2.029±0.018	1.992±0.010	1.925±0.018	1.896	0.612	0.052		

[*] Errors are 2σ for the regression only.; ** Errors are those at 95% confidence level for the regression only.; *** Number in parenthesis represents both errors at 95% confidence level for the regression and potential systematic bias.

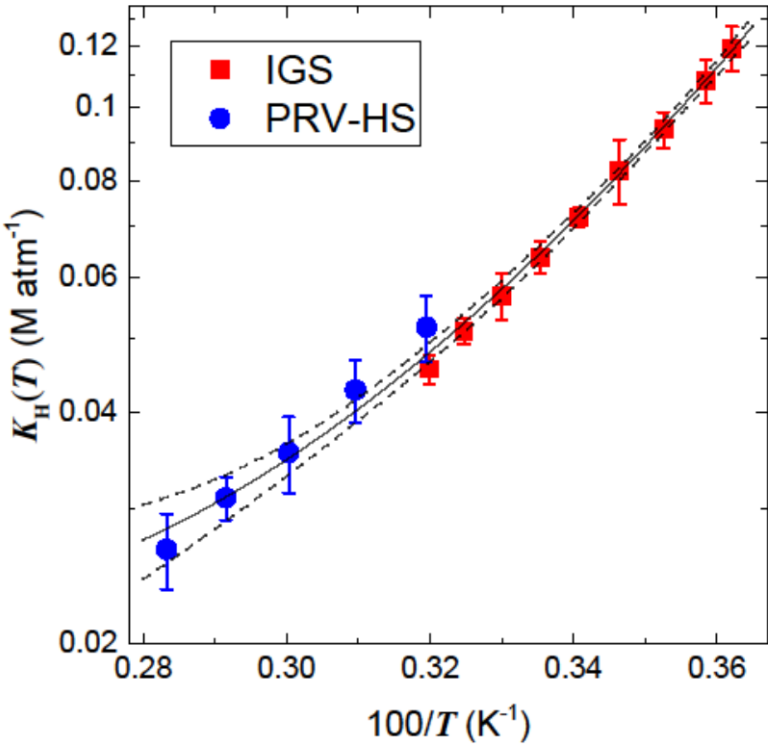

Figure 2m. van't Hoff plot of the K_H values obtained by the IGS method and the PRV-HS method. Bold curve displays the fitting of the data obtained by the IGS method and the PRV-HS method (Eq. (13)). Dashed curves display upper and lower 95% confidence limit of the above fitting by Eq. (12). Error bars of the data by the IGS method represent both 2σ for the average and potential systematic bias. Error bars of the data by PRV-HS method represent both errors at 95% confidence level for the regression and potential systematic bias.

R2. Reply to the comment 2 that there does appear to be a small – yet significant – offset between PRV-HS and IGS method in Figure 2 at 312 K and why IGS is believed to be more accurate.

Thank you for the comments.

There appears to be a small - yet significant - offset between PRV-HS and IGS method at 312 K. This point is also commented by Referee 1. For the PRV-HS methods, values of $\delta K_{eq}/K_{eq}$ may have potential systematic bias of ca. ±4%, which results mostly from the accuracy of temperature of the test solution, as aforementioned (R1. (2)). For the IGS method, values of $\delta K_{eq}/K_{eq}$ may have potential systematic bias of ca. ±2%. The IGS method is thus believed to be more accurate. Potential systematic bias in both the PRV-HS method and the IGS method could be a reason why there is the small offset between PRV-HS and IGS method at 312 K.

R3. Reply to the comment 3 on the fit according to Eq. (13)

Thank you for the comment.

The fit according to Eq. (13) does not take into account the relative weight of error bars.

R4. Reply to the comment 4 on the reason for the large variation in the size of error bars in Fig. 5.

Thank you for the comment.

As Referee 2 comments, there are the large variation in the size of error bars in Fig. 5. Ratio among error bars of the

data at the same temperature is up to the maximum value of 4.5: error bars are 0.084 for 8.921‰ and 0.019 for 51.534‰ at 10.5 °C. Error bars for the data at 8.921‰ tend to be large and error bars for the data at 51.534‰ tend to be small: this reflects statics errors of the data at 8.921‰ and 51.534‰.

Errors of the data in Fig. 5 represents statics only (Error_S). As replied in R1, errors from both statics (Error_S) and potential systematic bias of ±2% (Error_B) will be used as errors (Error_T) for the data in Fig. 5: (Error_T) = (Error_S) + (Error_B). Error bars of the data in Fig. 5m represent Error_T. As seen in Fig. 5m, the ratios among error bars of the data at the same temperature are smaller than the corresponding ratios in Fig. 5. For example, the ratio of error bars between at 8.921‰ and 51.534‰ at 10.5 °C is 2.7 while it is 4.5 in Fig. 5 as aforementioned.

In the revised manuscript, error bars will be represented by Error_T in Fig. 5m.

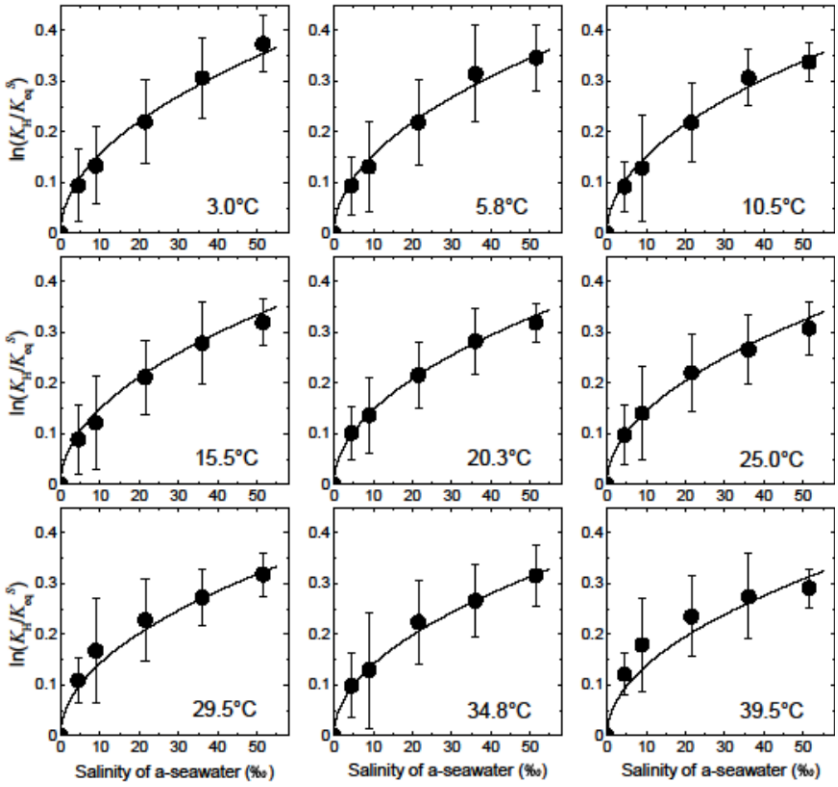

Figure 5m. Plots of $\ln(K_H(T)/K_H^S(T))$ vs. salinity in a-seawater at each temperature. Bold curves represent the fitting obtained by Eq. (22). Error bars represent errors reflecting both 2σ for the average and potential systematic bias of K_{eq}^S.

R5. Reply to the comment 5 on the discussion on the $S^{0.5}$ components of the fit (deviation from Setchenow).

Thank you for the comment.

The reason why $\ln(K_H/K_{eq}^S)$ is proportional to $S^{0.5}$ rather than S is still unclear.

I will describe a potential reason for this proportionality simply in the text, and make discussion in *Supporting Information* as follows.

L20-21, P9:

The reason for this salting-out effect of CH_2F_2 solubility in a-seawater is not clear. Specific properties of CH_2F_2 –small molecular volume, which results in small work of cavity creation (Graziano, 2004; 2008), and large solute-solvent attractive potential energy in water and a-seawater– may cause deviation from Setchenow relationship (*Supporting Information*).

In *Supporting Information*:

I will calculate Ben-Naim standard Gibbs energy $\Delta G^{\bullet}$, enthalpy $\Delta H^{\bullet}$, and entropy $\Delta S^{\bullet}$ changes for dissolution of CH_2F_2 in water because these values correspond to the values for the transfer from a fixed position in the gas phase to a fixed position in water. Values of $\Delta G^{\bullet}$, $\Delta H^{\bullet}$, and $\Delta S^{\bullet}$ are calculated on the basis of the Ostwald solubility coefficient, $L(T)$, as follows.

$$\ln(L(T)) = \ln\left(RTK_{\mathrm{eq}}{}^{S}(T)\right) \quad \text{(B1)}$$

$$\Delta G^{\cdot} = R'T\ln(L(T)) \quad \text{(B2)}$$

$$\Delta H^{\cdot} = -\frac{\partial}{\partial(1/T)}\left(\frac{\Delta G^{\cdot}}{T}\right) \quad \text{(B3)}$$

$$\Delta S^{\cdot} = \frac{\Delta H^{\cdot} - \Delta G^{\cdot}}{T} \quad \text{(B4)}$$

where both R and R' represent gas constant but their units are different: R = 0.0821 in atm dm^3 K^{-1} mol^{-1}; R' = 8.314 in J K^{-1} mol^{-1}.

Combining Eqs. (B1), (B2), (B3), and (B4) with Eqs. (14) and (15), $\Delta G^{\bullet}$ (kJ mol^{-1}), $\Delta H^{\bullet}$ (kJ mol^{-1}), and $\Delta S^{\bullet}$ (J mol^{-1} K^{-1}) are represented by ΔG_{sol} and ΔH_{sol} as follows:

$$\Delta G^{\cdot} = \Delta G_{\mathrm{sol}} + R'T\ln(RT) \quad \text{(B5)}$$

$$\Delta H^{\cdot} = \Delta H_{\mathrm{sol}} + R'T \quad \text{(B6)}$$

$$\Delta S^{\cdot} = \frac{\Delta H_{\mathrm{sol}} - \Delta G_{\mathrm{sol}}}{T} + R'T - R'T\ln(RT) \quad \text{(B7)}$$

Values of $\Delta G^{\bullet}$, $\Delta H^{\bullet}$, and $\Delta S^{\bullet}$ calculated at 298 K are listed in Table S2. Table S2 also lists values of $\Delta G^{\bullet}$, $\Delta H^{\bullet}$, and $\Delta S^{\bullet}$ reported for CH_3F and C_2H_6 (Graziano, 2004) and CH_4 (Graziano, 2008) at 298 K. The chemicals, which having a methyl group, in Table 2 are classified into two groups (CH_2F_2 and CH_3F; CH_4 and C_2H_6) according to $\Delta G^{\bullet}$.

Table S2. Ben-Naim standard hydration Gibbs energy $\Delta G^{\bullet}$, enthalpy $\Delta H^{\bullet}$, and entropy $\Delta S^{\bullet}$ changes for dissolution of CH_2F_2 at 298 K determined here and the corresponding values reported for CH_3F and C_2H_6 (Granziano, 2004) and CH_4 (Graziano, 2008).

	$\Delta G^{\cdot}$ (kJ mol^{-1})	$\Delta H^{\cdot}$ (kJ mol^{-1})	$\Delta S^{\cdot}$ (J K^{-1} mol^{-1})	ΔG_c (kJ mol^{-1})	E_a (kJ mol^{-1})	ΔH^h (kJ mol^{-1})
CH_2F_2	−1.1	−14.7	−45.4			
CH_3F	−0.9	−15.8	−50.0	23.3	−24.3	8.5
CH_4	8.4	−10.9	−64.7	22.9	−14.5	3.7
C_2H_6	7.7	−17.5	−84.5	28.4	−20.7	3.2

Table 2 lists values of ΔG_c, E_a and ΔH^h deduced using a scaled particle theory (Granziano, 2004; 2008). ΔG_c is the work of cavity creation to insert a solute in a solvent. E_a is a solute-solvent attractive potential energy and accounts for the solute-solvent interactions consisting of dispersion, dipole-induced dipole, and dipole-dipole contributions. ΔH^h is enthalpy of solvent molecules reorganization caused by solute insertion. The solvent reorganization mainly involves a rearrangement of H-bonds.

ΔG_c is entropic in nature in all liquids, being a measure of the excluded volume effect due to a reduction in the spatial configurations accessible to liquid molecules upon cavity creation. Hence, C_2H_6 has larger value of ΔG_c than CH_3F and CH_4. ΔG_c, E_a, and ΔH^h are related to $\Delta G^{\bullet}$ and $\Delta H^{\bullet}$ as follows (Graziano, 2008):

$$\Delta G^{\cdot} = \Delta G_c + E_a \quad \text{(B8)}$$

$$\Delta H^{\cdot} = E_a + \Delta H^h \quad \text{(B9)}$$

Table S10m thus suggests that smaller value of $\Delta G^{\bullet}$ of CH_3F than CH_4 is due to large solute-solvent attractive potential energy ($-E_a$) of CH_3F.

Graziano (2008) definitively explained the salting-out of CH_4 by sodium chloride at molecular level on the basis of a

scaled particle theory. He explained that $\Delta G^{\bullet}$ increase was linearly related to the increase in the volume packing density of the solutions (ξ_3) with adding NaCl. Such a increase of $\Delta G^{\bullet}$ is probably the case for salting-out of CH_2F_2 by a-seawater observed in this study. He also explained that E_a was linearly related to the increase in ξ_3 assuming that a fraction of the dipole-induced dipole attractions could be taken into account by the parameterization of the dispersion contribution.

I think the possibility that E_a may be nonlinearly related to the increase in ξ_3 because of dipole-dipole interaction between CH_2F_2 and solvents. Temperature dependence in Eq. (23) suggests that salting-out effect of CH_2F_2 by a-seawater is enthalpic. Eqs. (23) and (B9) thus suggests that the salting-out of CH_2F_2 is mostly related to change in E_a. CH_2F_2 has relatively small value of ΔG_c because of its small molecular volume compared to other chemicals such as C_2H_6. Accordingly, $\Delta G^{\bullet}$, that is, solubility of CH_2F_2 would depend on E_a rather than ΔG_c. Therefore, I think that specific properties of CH_2F_2 –small molecular volume, which results in small work of cavity creation (Graziano, 2004; 2008), and large solute-solvent attractive potential energy in water and a-seawater– may cause deviation from Setchenow relationship.

The following two references will be cited both in the manuscript and in *Supporting Information*.

Graziano, G.: Case study of enthalpy–entropy noncompensation. Journal of Chemical Physics, 120, 4467-4471, doi: 10.1063/1.1644094, 2004.

Graziano, G.: Salting out of methane by sodium chloride: A scaled particle theory study. Journal of Chemical Physics, 129, 084506, doi: 10.1063/1.2972979, 2008.

R6. Reply to the comments 6: how deep is this mixed ocean layer in the model? Does this mean the model estimates an upper limit?

Thank you for the comments.

The depth of the ocean mix layer in the model is 10 to 600 m. The depth distribution of CH_2F_2 dissolved in the ocean mixed layer in each semi-hemisphere is listed in Tables S3 (30° S–90° S), S4 (30° S–0° S), S5 (0° N–30° S) and S6 (30° N–90° N). As seen in these tables, the CH_2F_2 dissolved in the ocean mixed layer resides mostly in less than 300 m depth. For example, for the southern semi-hemisphere (30° S–90° S) (Table S3), in August, when the amount of CH_2F_2 dissolved in the ocean mixed layer is maximum, 66% of the CH_2F_2 dissolved in the mixed layer would reside between 200 m and 300 m depth, and 91 % of the CH_2F_2 dissolved in the ocean mixed layer is expected to reside in less than 300 m depth.

As Referee 2 pointed out, model estimates mean an upper limit of the amount of CH_2F_2 dissolved in the ocean mixed layer. This point will be clearly described in the revised manuscript as follows.

P10, L23:

As seen in Figure 6, in the southern semi-hemispheric lower troposphere (30° S−90° S), at least 5 % of the atmospheric burden of CH_2F_2 would reside in the ocean mixed layer in the winter, and the annual variance of the CH_2F_2 residence ratio would be 4%. These ratios are, in fact, upper limits because CH_2F_2 in the ocean mixed layer may be undersaturated. It takes days to a few weeks after a change in temperature or salinity for oceanic surface mixed layers to come to equilibrium with the present atmosphere, and equilibration time increases with depth of the surface mixed layer (Fine, 2011). In the estimation using the gridded data here, >90 % of CH_2F_2 in the ocean mixed layer would reside in less than 300 m depth (Tables S3, S4, S5 and S6).

Haine and Richards (1995) demonstrated that seasonal variation in ocean mixed layer depth was the key process which affected undersaturation and supersaturation of chlorofluorocarbon 11 (CFC-11), CFC-12 and CFC-113 by use of a one-dimensional slab mixed model. As described above, >90 % of CH_2F_2 in the ocean mixed layer is expected to reside in less than 300 m depth. According to the model calculation results by Haine and Richards (1995), saturation of CH_2F_2 would

be >0.9 for the ocean mixed layer with less than 300 m depth. The saturation of CH_2F_2 in the ocean mixed layer is thus estimated to be at least 0.8. In the southern semi-hemispheric lower troposphere (30° S–90° S), therefore, at least 4 % of the atmospheric burden of CH_2F_2 would reside in the ocean mixed layer in the winter, and the annual variance of the CH_2F_2 residence ratio would be 3%.

The following two references will be cited in the manuscript.

Fine, R. A.: Observations of CFCs and SF_6 as ocean tracers. Annual Review of Marine Science, 3, 173-195, doi:10.1146/annurev.marine.010908.163933, 2011.

Haine, T. W. N. and Richards, K. J.: The influence of the seasonal mixed layer on oceanic uptake of CFCs. Journal of Geophysical Research, 100, 10727-10744, doi:10.1029/95JC00629, 1995.

Table S3. Monthly amount of CH_2F_2 dissolved in the ocean mixed layer at solubility equilibrium with the atmospheric CH_2F_2 (1 patm) and the depth distribution of the CH_2F_2 dissolved in the southern semi-hemisphere (90°S - 30°S).

	Amount (Gg patm^{-1})	Depth distribution of CH_2F_2 dissolved in the ocean mixed layer (%)					
		10 - 100 m	100 - 200 m	200 - 300 m	300 - 400 m	400 - 500 m	500 - 600 m
January	0.0169	94.9	2.9	1.0	0.5	0.3	0.3
February	0.0201	92.1	3.6	2.9	1.0	0.3	0.0
March	0.0255	87.8	9.2	1.7	0.7	0.2	0.4
April	0.0338	66.5	31.8	1.1	0.2	0.1	0.2
May	0.0409	48.5	48.1	2.2	0.8	0.3	0.0
June	0.0510	26.8	62.7	8.0	1.7	0.8	0.1
July	0.0571	14.1	69.3	12.2	3.3	0.9	0.1
August	0.0640	8.5	65.8	17.0	6.2	2.3	0.2
September	0.0609	13.5	61.0	14.6	8.2	2.7	0.0
October	0.0504	24.7	58.6	12.1	2.9	1.4	0.3
November	0.0335	60.4	30.5	4.6	2.2	2.3	0.1
December	0.0196	95.1	4.3	0.4	0.2	0.0	0.0

Table S4. Monthly amount of CH_2F_2 dissolved in the ocean mixed layer at solubility equilibrium with the atmospheric CH_2F_2 (1 patm) and the depth distribution of the CH_2F_2 dissolved in the southern semi-hemisphere (30°S - 0°S).

	Amount (Gg patm^{-1})	Depth distribution of CH_2F_2 dissolved in the ocean mixed layer (%)					
		10 - 100 m	100 - 200 m	200 - 300 m	300 - 400 m	400 - 500 m	500 - 600 m
January	0.0084	99.6	0.4	0	0	0	0
February	0.0084	99.7	0.3	0	0	0	0
March	0.0089	100.0	0	0	0	0	0
April	0.0106	100.0	0	0	0	0	0
May	0.0131	100.0	0	0	0	0	0
June	0.0163	97.1	2.9	0	0	0	0
July	0.0189	80.1	19.9	0	0	0	0
August	0.0193	73.1	26.9	0	0	0	0
September	0.0165	82.2	17.8	0	0	0	0
October	0.0124	94.6	5.4	0	0	0	0
November	0.0097	99.9	0.1	0	0	0	0
December	0.0087	100.0	0	0	0	0	0

Table S5. Monthly amount of CH_2F_2 dissolved in the ocean mixed layer at solubility equilibrium with the atmospheric CH_2F_2 (1 patm) and the depth distribution of the CH_2F_2 dissolved in the southern semi-hemisphere (0°N - 30°N).

	Amount (Gg patm^{-1})	Depth distribution of CH_2F_2 dissolved in the ocean mixed layer (%)					
		10 - 100 m	100 - 200 m	200 - 300 m	300 - 400 m	400 - 500 m	500 - 600 m
January	0.0132	96.4	3.6	0	0	0	0
February	0.0126	95.9	4.1	0	0	0	0
March	0.0107	98.7	1.3	0	0	0	0
April	0.0087	99.8	0.2	0	0	0	0
May	0.0079	100.0	0	0	0	0	0
June	0.0080	100.0	0	0	0	0	0
July	0.0084	100.0	0	0	0	0	0
August	0.0082	100.0	0	0	0	0	0
September	0.0080	100.0	0	0	0	0	0
October	0.0086	100.0	0	0	0	0	0
November	0.0100	100.0	0	0	0	0	0
December	0.0118	100.0	0	0	0	0	0

Table S6. Monthly amount of CH_2F_2 dissolved in the ocean mixed layer at solubility equilibrium with the atmospheric CH_2F_2 (1 patm) and the depth distribution of the CH_2F_2 dissolved in the southern semi-hemisphere (30°N - 90°N).

	Amount (Gg patm^{-1})	Depth distribution of CH_2F_2 dissolved in the ocean mixed layer (%)					
		10 - 100 m	100 - 200 m	200 - 300 m	300 - 400 m	400 - 500 m	500 - 600 m
January	0.0205	41.3	50.1	7.0	1.4	0.2	0.0
February	0.0225	34.5	55.3	7.1	2.3	0.6	0.2
March	0.0208	49.7	42.3	4.9	1.7	0.7	0.6
April	0.0147	79.7	17.6	1.7	0.4	0.0	0.6
May	0.0081	90.1	9.9	0	0	0	0
June	0.0055	97.7	2.3	0	0	0	0
July	0.0045	96.6	3.4	0	0	0	0
August	0.0048	94.4	5.6	0	0	0	0
September	0.0059	97.7	2.3	0	0	0	0
October	0.0084	99.6	0.4	0	0	0	0
November	0.0121	89.6	10.4	0.1	0	0	0
December	0.0163	71.0	26.1	2.9	0	0	0

R7. Reply to the comment 7 on how much departure from saturation equilibrium the oceanic mixed layer in the model is.

Thank you for the comment.

As described in R6, it takes days to a few weeks after a change in temperature or salinity for oceanic surface mixed layers to come to equilibrium with the present atmosphere, and equilibration time increases with depth of the surface mixed layer (Fine, 2011).

Haine and Richards (1995) demonstrated that the seasonal variation in ocean mixed layer depth was the key process which affected undersaturation and supersaturation of chlorofluorocarbon 11 (CFC-11), CFC-12 and CFC-113 by use of a one-dimensional slab mixed model. Specifically, the mixed layer deepening in autumn would cause undersaturation in the mixed layer. In the estimation, >90 % of CH_2F_2 in the ocean mixed layer is expected to reside in less than 300 m depth (Tables S3, S4, S5 and S6). According to the report by Haine and Richards (1995), saturation of CH_2F_2 would be >0.9 for the ocean mixed layer with less than 300 m depth. The saturation of CH_2F_2 in the ocean mixed layer is thus estimated to be at least 0.8.

The manuscript will be revised, as described in R6, and Fine (2011) and Haine and Richards (1995) will be cited.

R8. Replay to the comment 8 on how the dissolution of CH_2F_2 into the ocean should affect estimation of CH_2F_2 emissions in the Southern Hemisphere and their seasonal variability.

Thank you for the comment.

As Referee 2 pointed out, the atmospheric concentrations that reach the Southern Hemisphere are also affected by transport, chemical removal, and related uncertainties; this should be mentioned.

I will first describe how the dissolution of CH_2F_2 into the ocean may affect estimation of CH_2F_2 emissions in the Southern Hemisphere and their seasonal variability, and then I will show the revised text.

In 2012, atmospheric concentrations of CH_2F_2 in the Northern Hemisphere are by >30% higher than in the Southern Hemisphere (O'Doherty et al., 2014); the strong inter-hemisphere gradient indicates that emissions of CH_2F_2 are predominantly in the Northern Hemisphere. In the AGAGE 12 box model (Rigby et al., 2013), transport of CH_2F_2 is dominated by eddy diffusion between the boxes in the model. The seasonal eddy diffusion parameters between the Northern Hemisphere and the Southern Hemisphere in the model are 187 to 568 days in lower troposphere, and 81 to 109 days in upper troposphere (Rigby et al., 2013).

The rate of increase in atmospheric concentration of CH_2F_2 due to the emission of CH_2F_2 in the Southern Hemisphere, which is denoted as RE_{south} hereafter, is thus more sensitive to change in atmospheric concentrations of CH_2F_2 in the Southern Hemisphere than those in the Northern Hemisphere, partly because CH_2F_2 is removed through gas phase reactions with OH (partial atmospheric lifetime of 5.5 years). Furthermore, RE_{south} would range small values such as a few % y^{-1} or less because emissions of CH_2F_2 are predominantly in the Northern Hemisphere and because, in 2012, the rate of increase in the global mean mole fraction of CH_2F_2 was 17% y^{-1} (O'Doherty et al., 2014). In estimation of RE_{south}, small value of RE_{south} would be deduced from difference in the rates of increase of atmospheric concentrations of CH_2F_2 between hemispheres. Dissolution of CH_2F_2 in the ocean in the Southern Hemisphere may thus affect estimation of RE_{south} and then affect estimation of CH_2F_2 emissions in the Southern Hemisphere and their seasonal variability.

I will revise the text as follows.

L26-29, P10:

Hence, dissolution of CH_2F_2 in the ocean, even if dissolution is reversible, may influence estimates of CH_2F_2 emissions derived from long-term observational data on atmospheric concentrations of CH_2F_2; in particular, consideration of dissolution of CH_2F_2 in the ocean may affect estimates of CH_2F_2 emissions in the Southern Hemisphere and their seasonal variability because of slow rates of inter-hemispheric transport and small portion of the CH_2F_2 emissions in the Southern Hemisphere to the total emissions.

Specific comments:

P2, L28: 'first' is written twice.

Thank you for the comment.

The text is revised as follows.

First, the values of K_H for CH_2F_2 were determined over the temperature range from 276 to 313 K by means of an inert-gas stripping (IGS) method.

P5, L8: add errors for numbers. Add typical values, their units, and uncertainties of variables for the key equations throughout the manuscript.

Thank you for the comment.

If redistribution of CH_2F_2 in the headspace to the test solution had occurred, the K_H values determined in this study would be overestimated. Errors due to this redistribution are always negative values. The ratio of the errors to the K_{eq} values (%) is $100 \times \frac{\left(\frac{V_{head}}{RTV}\right)}{\left(\frac{1}{k_1 RTV}\right)}$, that is, $\frac{100 k_1 V_{head}}{F}$. Under the experimental conditions here, this ratio is calculated to be −2.0 to −2.3 % at 3.0 °C and −4.6 to −5.1 % at 39.5 °C. Values of this ratio increase as values of K_{eq} decrease. This ratio is maximum (−6.5 %) for a-seawater at 51.534‰ and 39.5 °C.

Typical values, their units, and uncertainties of variables for the key equations are added as follows.

L6-8, P4:

The solution was magnetically stirred, and its temperature was kept constant within ±0.2 K by means of a constant-temperature bath that had both heating and cooling capabilities (NCB-2500, EYELA, Tokyo, Japan) and was connected to the water jacket of the column.

L14-16, P4:

The volumetric flow rate of the gas (F_{meas}) was calibrated with a soap-bubble meter for each experimental run. The soap-bubble meter had been calibrated by means of a high-precision film flow meter SF-1U with VP-2U (Horiba, Kyoto, Japan). Errors of F_{meas} are within ±1%.

L18-19, P4:

All volumetric gas flows were corrected to prevailing temperature and pressure by Eq. (3) (Krummen et al., 2000). Errors due to this correction are within ±1%. Errors of F are thus within ±1.4%.

L13, P5:

Hence Eq. (6) was used to deduce $K_{eq}(T)$ from k_1. If redistribution of CH_2F_2 in the headspace to the test solution had occurred, the values determined using Eq. (6) would be overestimated. Errors due to this redistribution are always negative values. Ratio of the errors to the K_{eq} values (%) is $\frac{100 k_1 V_{head}}{F}$. Values of this ratio increase as values of K_{eq} decrease. Under the experimental conditions here, this ratio is calculated to be from –2.0 % for water at 3.0 °C to −6.5 % for a-seawater at 51.534‰ and 39.5 °C.

L27, P7, Eq. (13):

$$\ln(K_H(T)) = -49.71 + 77.70 \times \left(\frac{100}{T}\right) + 19.14 \times \ln\left(\frac{T}{100}\right) \qquad (13)$$

The square-root-of-variance, that is, standard deviation for each fitting coefficient in Eq. (12) is as follows:

$\delta a_1 = 5.5$; $\delta a_2 = 8.3$; $\delta a_3 = 2.8$.

L10-L26, P9:

This result suggests that $\ln(K_H(T)/K_{eq}^S(T))$ varied according to Eq. (18):

$$\ln(K_H(T)/K_{eq}^S(T)) = k_{s1} S^{0.5} \qquad (18)$$

Values of k_{s1} may be represented by the following function of T:

$$k_{s1} = b_1 + b_2 \times (100/T) \qquad (19)$$

Parameterizations of b_1 and b_2 obtained by fitting all the $\ln(K_H(T)/K_{eq}^S(T))$ and S data at each temperature simultaneously by

means of the nonlinear least-squares method gives Eq. (20).

$$\ln(K_H(T)/K_{eq}^S(T)) = (0.0127 + 0.0099 \times (100/T)) \times S^{0.5} \quad (20)$$

The standard deviation for each fitting coefficient in Eq. (19) is as follows:

$\delta b_1 = 0.0106$; $\delta b_2 = 0.0031$.

Since $2\times\delta b_1 > b_1$, the parameterization by Eq. (19) may be overworked. Accordingly, all the $\ln(K_H(T)/K_{eq}^S(T))$ and S data at each temperature are fitted simultaneously using Eq. (21) instead of Eq. (19). The nonlinear least-squares method gives Eq. (22).

$$k_{s1} = b_2 \times (100/T) \quad (21)$$

$$\ln(K_H(T)/K_{eq}^S(T)) = 0.1343 \times (100/T) \times S^{0.5} \quad (22)$$

The standard deviation for the fitting coefficient in Eq. (21) is as follows: $\delta b_2 = 0.0013$. As seen in Fig. 5, Eqs. (21) and (22) reproduced the data well.

$\ln(K_H(T)/K_{eq}^S(T))$ depends on $S^{0.5}$ and follows Eq. (22) rather than the Setchenow dependence (Eq. (17)). Table S7 compares values of K_{eq}^S calculated by Eq. (22) with those by Eq. (17). The difference between these values of K_{eq}^S at 35‰ of salinity was within 3% of the K_{eq}^S value. Decreases in values of K_{eq}^S are calculated to be 7–8% and 4%, respectively, by Eqs. (17) and (23) as salinity of a-seawater increases from 30‰ to 40‰ at each temperature.

The reason for this salting-out effect of CH_2F_2 solubility in a-seawater is not clear. Specific properties of CH_2F_2 –small molecular volume, which results in small work of cavity creation (Graziano, 2004; 2008), and large solute-solvent attractive potential energy in water and a-seawater– may cause deviation from Setchenow relationship (*Supporting Information*).

In Eq. (22), $K_H(T)$ is represented by Eq. (13), as described in Sect. 3.1. Therefore $K_{eq}^S(T)$ is represented by Eq. (23):

$$\ln(K_{eq}^S(T)) = -49.71 + (77.70 - 0.1343 \times S^{0.5}) \times (100/T) + 19.14 \times \ln(T/100) \quad (23)$$

The values calculated with Eq. (23) are indicated by the bold curves in Fig. 4 and are listed in Table 3. Equation (23) reproduced the experimentally determined values of $K_H(T)$ and $K_{eq}^S(T)$ within the uncertainty of these experimental runs.

P7, L6: What statistical test for outliers was applied? How many points were removed at each temperature.

Thank you for the comment.

Statistical test for outliers is as follows.

The data with errors being >10% of the data was first excluded. Next, some data were excluded for calculation of the average so that the remaining data were inside the 2σ range. This procedure was iterated until all the data were inside the 2σ range.

The data points thus excluded was only for V values of 0.350 dm^3. The number of them were eight or fewer at each temperature. The maximum number of the data excluded was corrected to be eight although it was described to be six in the original manuscript. Number of the data thus excluded were indicated in Tables 1m (shown in R1) and 3m.

Table 3m. The average of values of $F/(k_1RTV)$ obtained for V value of 0.350 dm^3 and the $K_{eq}^S(T)$ value derived from Eq. (23) at each salinity and temperature. N represents number of experimental runs for the average.

T (K)	K_{eq}^S (M atm^{-1})					
	salinity, 4.452 ‰			salinity, 8.921 ‰		
	average [a, b]	N [c]	Eq. (23)	average [a, b]	N [c]	Eq. (23)
276.15	0.108 ± 0.006 (0.008)	8 (0)	0.108	0.103 ± 0.006 (0.008)	21 (0)	0.104
278.35	0.099 ± 0.004 (0.006)	12 (0)	0.099	0.095 ± 0.006 (0.008)	26 (1)	0.095
283.65	0.086 ± 0.003 (0.005)	9 (0)	0.085	0.083 ± 0.007 (0.009)	24 (0)	0.082
288.65	0.075 ± 0.004 (0.006)	12 (0)	0.074	0.072 ± 0.005 (0.006)	33 (0)	0.071
293.45	0.065 ± 0.002 (0.003)	10 (0)	0.065	0.063 ± 0.003 (0.004)	27 (5)	0.062
298.15	0.058 ± 0.002 (0.003)	13 (0)	0.058	0.056 ± 0.004 (0.005)	26 (2)	0.056
303.05	0.052 ± 0.001 (0.002)	8 (0)	0.052	0.049 ± 0.004 (0.005)	14 (6)	0.050
307.95	0.047 ± 0.002 (0.003)	13 (1)	0.047	0.046 ± 0.004 (0.005)	23 (1)	0.045
312.65	0.042 ± 0.001 (0.002)	7 (0)	0.042	0.040 ± 0.003 (0.004)	12 (8)	0.041

T (K)	K_{eq}^S (M atm^{-1})					
	salinity, 21.520 ‰			salinity, 36.074 ‰		
	average [a, b]	N [c]	Eq. (23)	average [a, b]	N [c]	Eq. (23)
276.15	0.095 ± 0.006 (0.008)	20 (0)	0.095	0.088 ± 0.005 (0.007)	21 (0)	0.088
278.35	0.087 ± 0.005 (0.007)	22 (0)	0.087	0.079 ± 0.006 (0.008)	20 (3)	0.081
283.65	0.075 ± 0.004 (0.006)	15 (1)	0.076	0.069 ± 0.002 (0.003)	18 (2)	0.071
288.65	0.066 ± 0.004 (0.005)	20 (0)	0.066	0.062 ± 0.004 (0.005)	19 (4)	0.062
293.45	0.058 ± 0.003 (0.004)	14 (0)	0.058	0.054 ± 0.002 (0.003)	19 (4)	0.055
298.15	0.052 ± 0.003 (0.004)	20 (0)	0.052	0.049 ± 0.002 (0.003)	24 (4)	0.049
303.05	0.046 ± 0.003 (0.004)	16 (0)	0.046	0.044 ± 0.002 (0.003)	16 (0)	0.044
307.95	0.042 ± 0.003 (0.004)	16 (0)	0.042	0.040 ± 0.002 (0.003)	15 (2)	0.040
312.65	0.038 ± 0.002 (0.003)	16 (0)	0.038	0.036 ± 0.002 (0.003)	16 (0)	0.037

T (K)	K_{eq}^S (M atm^{-1})		
	salinity, 51.534 ‰		
	average [a, b]	N [c]	Eq. (23)
276.15	0.081 ± 0.003 (0.005)	10 (0)	0.082
278.35	0.077 ± 0.003 (0.005)	15 (0)	0.076
283.65	0.067 ± 0.001 (0.003)	9 (1)	0.066
288.65	0.059 ± 0.002 (0.003)	14 (1)	0.058
293.45	0.052 ± 0.001 (0.002)	7 (3)	0.052
298.15	0.047 ± 0.002 (0.003)	15 (0)	0.047
303.05	0.042 ± 0.001 (0.002)	8 (0)	0.042
307.95	0.038 ± 0.002 (0.003)	12 (0)	0.039
312.65	0.036 ± 0.001 (0.002)	7 (1)	0.036

a. Errors are 2σ for the average only.; b. Number in parenthesis represents an error reflecting both 2σ for the average and potential systematic bias.; c. Number in parenthesis represents number of experimental runs excluded for the average.

Eq (17). For sake of discussion, can a k_S value be given here? And what is the effect of including k_S vs k_{S1}, k_{S2} in the model - does it make a difference?

Thank you for the comment.

In Table S7, values of k_s were given, and the K_{eq} values calculated by Eq. (17) were compared to those by Eq. (22) at salinity of 30, 35 and 40 ‰ and each temperature. The text on lines 6-8 and lines 20-21 in page 9 will be revised as follows.

L6-8, P9:

Figure 5 plots $\ln(K_H(T)/K_{eq}^S(T))$ against S at each temperature. Table S7 lists values of k_s determined by fitting the data at each temperature by use of Eq. (17). If the $K_{eq}^S(T)$ values obeyed Eq. (17), the data at each temperature in Fig. 5 would fall on a straight line passing through the origin, but they did not. Figure 5 reveals that the salinity dependence of CH_2F_2 solubility in a-seawater cannot be represented by Eq. (17).

L20-21, P9:

$\ln(K_H(T)/K_{eq}^S(T))$ depends on $S^{0.5}$ and follows Eq. (22) rather than the Setchenow equation (Eq. (17)). Table S14m lists ratios of K_{eq}^S calculated by Eq. (17) to those by Eq. (22). Difference between values of K_{eq}^S calculated by Eqs. (17) and (22) at 35‰ of salinity was within 3% of the K_{eq}^S value. Decreases in values of K_{eq}^S are calculated to be 7–8% and 4%, respectively, by Eqs. (17) and (23) as salinity of a-seawater increases from 30‰ to 40‰ at each temperature.

The reason for this salting-out effect of CH_2F_2 solubility in a-seawater is not clear.

Table S7. Values of k_s (Eq. (17)) and comparison of values of K_{eq}^S calculated at each temperature by Eq. (17) with those by Eq. (22).

Temperature (°C)	k_s ($‰^{-1}$)	[K_{eq}^S from Eq. (17)]/ [K_{eq}^S from Eq. (22)]			[K_{eq}^S at 30‰]/ [K_{eq}^S at 40‰]	
		at 30‰	at 35‰	at 40‰	Eq. (17)	Eq. (23)
3.0	0.00811	1.027	1.008	0.988	1.084	1.043
5.8	0.00785	1.033	1.014	0.995	1.082	1.042
10.5	0.00768	1.033	1.016	0.997	1.080	1.042
15.5	0.00718	1.044	1.028	1.012	1.074	1.041
20.3	0.00728	1.037	1.020	1.003	1.076	1.040
25.0	0.00704	1.040	1.024	1.008	1.073	1.039
29.9	0.00731	1.027	1.010	0.992	1.076	1.039
34.8	0.00713	1.029	1.012	0.995	1.074	1.038
39.5	0.00709	1.026	1.010	0.992	1.073	1.038